Nonlinear Regulation of End-Effector Motion for a Flexible Robot Arm

A. De Luca, L. Lanari, G. Ulivi

Abstract

In this paper we consider the problem of controlling via state-feedback the end-effector motion of a one-link flexible robot arm described by a nonlinear dynamic model. Due to the non-minimum phase nature of the system zero-dynamics, use of pure inversion-based techniques is unfeasible. In order to obtain stable tracking of desired tip trajectories, a nonlinear regulation approach is followed. Alternate general design procedures that exploit system invertibility are presented, leading to regulators of different complexity and real-time demand. Issues about the generation of output reference trajectories and the off-line computation of the associated steady-state trajectories are discussed, using the one-link flexible arm as a case study. Simulation results obtained for a spline trajectory and for a point-to-point motion show the achievable tracking accuracy and the wide applicability of the presented control technique.

Introduction

The most simple approach to the problem of output tracking in nonlinear systems is based on input-output inversion techniques [1,2]. In robotics, this solution has been applied for exact reproduction of joint and end-effector trajectories, both in rigid manipulators [3] and in robots with rigid links and elastic joints [4]. The main feature of these invertible systems is that no zero-dynamics is present, and so full linearization can be obtained by means of nonlinear static or, when needed, dynamic state feedback [5]. In this case, use of an inverse control law induces no unobservable part in the closed-loop system.

More in general, the feasibility of an inversion-based approach relies on the assumption of asymptotic stability of the zero-dynamics [6] associated to the system — which in the linear SISO case is equivalent to assuming a minimum phase transfer function. Under this hypothesis, the obtained closed-loop system consists of an input-output linear and controllable part, and of an unobservable but stable dynamics. Instead, when the zero-dynamics is unstable, inverse control substantially leads to an unbounded state evolution in the closed loop. In practice, the applied model-based input will saturate and output tracking will be completely lost. A different approach is then required for this class of nonlinear systems in order to obtain trajectory tracking *with* internal stability, i.e. output regulation. Recently, Isidori and Byrnes [7] have found a complete solution to the regulation problem for general nonlinear systems. Output tracking is achieved without forcing linearity in the input-output map through inversion; thus, this approach is suitable for asymptotic trajectory reproduction also in nonlinear non-minimum phase systems.

The presence of link flexibility in lightweight robotic systems turns the trajectory tracking problem into a less trivial one. Interestingly, both asymptotically stable and unstable zero-dynamics are encountered in this case. It is easy to show that trajectories defined at the *joint* level can be exactly reproduced in a stable fashion, using (static) inverse control [8]. On the other hand, pure inversion is not feasible for the execution of a desired *end-effector* motion, i.e. when the arm tip is required to follow a specified trajectory. In fact, for a robot with flexible links, the zero-dynamics associated with any reasonable definition of an output characterizing its end-effector location is unstable.

The non-minimum phase nature of end-effector motion is well known in one-link flexible robots [9-11], and is present in the relative dynamic model independently of its accuracy — nonlinear or linear, infinite or finite, with any number of elastic modes. The same characteristics are indeed inherited in the multi-link flexible case. Most of recent research is focused on one-link flexible arms, because of the control difficulties that already arise in this case. However, the problem of end-effector trajectory reproduction is rarely addressed [10-12]. A non-causal solution has been provided in [11], based on a frequency

approach and using a linear dynamic model of the arm. In [12], we have considered a simple nonlinear model, with flexibility concentrated in elastic springs along the link, and the problem was solved using nonlinear regulation theory for the first time. In particular, asymptotically exact tracking was obtained for sinusoidal tip motion and with a fourth-order dynamic model of the arm. Also, it was shown how the sinusoidal velocity profile could be used to produce a convenient end-effector trajectory of given time period.

In this paper, some alternatives in the design of nonlinear regulators are presented for a class of invertible systems. We consider different feedforward/feedback combinations, which are obtained by taking advantage of the existence of an input-output inversion — although destabilizing — control law. *Direct*, *indirect* and *mixed* designs are compared with respect to practical tracking performance and ease of implementation. This analysis provides the basis for bringing the nonlinear regulation approach into action even in more complex robotic applications, well beyond the simple example presented here. Proceeding as in [12], we demonstrate the feasibility of accurate output tracking even for trajectories generated by exosystems which do not satisfy the hypothesis assumed in [7]. Numerical simulations indicate that very limited transient errors can be obtained with the indirect nonlinear regulator in the case of cubic spline tip trajectories. Finally, results are reported for a point-to-point (rest-to-rest) move, in order to illustrate the wide applicability of the presented technique, which provides also new insight into classical cases.

Output Tracking via Nonlinear Regulation

Achieving exact or asymptotic tracking for a class of output trajectories while preserving stability in the closed-loop system is a classical regulation problem. The key idea for the solution is to find a bounded evolution of the state which produces the given output reference trajectory. The regulator will then drive the actual state towards this particular evolution, labeled *steady-state* for obvious reasons, asymptotically obtaining stable trajectory reproduction. Under mild assumptions, necessary and sufficient conditions were found in [7] for solving this problem in the case of nonlinear systems. These conditions are briefly recalled first. Consider a system defined by

$$\dot{\mathbf{x}} = \mathbf{f}(\mathbf{x}) + \mathbf{g}(\mathbf{x})\mathbf{u}, \qquad \mathbf{y} = \mathbf{h}(\mathbf{x}), \tag{1}$$

and assume that its linear approximation at $\mathbf{x} = \mathbf{0}$ is stabilizable by means of a linear state feedback $\mathbf{u} = \mathbf{F}\mathbf{x}$. A reference trajectory $\mathbf{y}_d(t)$ is supposed to be generated by an autonomous dynamic system (i.e. an *exosystem*)

$$\dot{\mathbf{w}} = \mathbf{s}(\mathbf{w}), \qquad \mathbf{y}_d = \mathbf{q}(\mathbf{w}), \tag{2}$$

for which every point in an open neighborhood of the stable equilibrium $\mathbf{w} = \mathbf{0}$ is Poisson stable (see [7]). Vector functions $\mathbf{f}$ and $\mathbf{h}$ are assumed to be zero at $\mathbf{x} = \mathbf{0}$, as well as $\mathbf{s}$ and $\mathbf{q}$ at $\mathbf{w} = \mathbf{0}$. Note that the assumption of Poisson stability considerably narrows the admissible class of dynamical systems eligible as trajectory generators. Indeed, this hypothesis is strictly required only when considering an unlimited time horizon, and may be relaxed when the reference trajectory to be reproduced is sufficiently well behaved, as will be shown in the case study on the flexible arm. A state feedback law of the form

$$\mathbf{u} = \mathbf{c}(\mathbf{w}) + \mathbf{F}\big(\mathbf{x} - \pi(\mathbf{w})\big), \tag{3}$$

with smooth $\mathbf{c}(\mathbf{w})$ and $\pi(\mathbf{w})$, $\mathbf{c}(\mathbf{0}) = \mathbf{0}$, and $\pi(\mathbf{0}) = \mathbf{0}$, solves the regulation problem if and only if $\mathbf{c}(\mathbf{w})$ and $\pi(\mathbf{w})$ satisfy the following equations:

$$\begin{aligned} \frac{\partial \pi}{\partial \mathbf{w}}\mathbf{s}(\mathbf{w}) &= \mathbf{f}(\pi(\mathbf{w})) + \mathbf{g}(\pi(\mathbf{w}))\mathbf{c}(\mathbf{w}), \\ \mathbf{q}(\mathbf{w}) &= \mathbf{h}(\pi(\mathbf{w})). \end{aligned} \tag{4}$$

The resulting nonlinear regulator (3) is made of a feedforward term $\mathbf{c}(\mathbf{w})$, providing the desired steady-state response, and of a linear feedback that is designed around the invariant manifold $\mathbf{x} = \pi(\mathbf{w})$ in the extended state space $(\mathbf{x}, \mathbf{w})$. Note that when $\mathbf{x} = \pi(\mathbf{w})$, $\mathbf{y} = \mathbf{y}_d$ necessarily follows. Also, if the initial state $\mathbf{x}(0)$ lies on the steady-state manifold associated with the desired output trajectory (i.e. $\mathbf{x}(0) = \pi(\mathbf{w}(0))$), exact output tracking will result. Otherwise, only asymptotic tracking is obtained, still with bounded internal

state. The overall block diagram of this *direct* regulator is reported in Fig. 1.

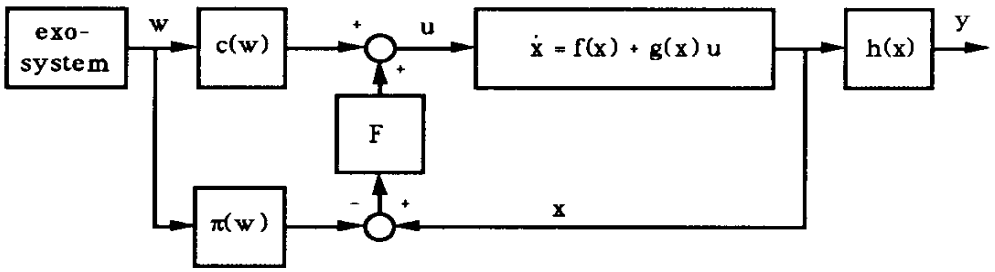

Fig. 1 — Nonlinear regulator: direct design

In the following two further schemes that realize the same nonlinear regulation concept will be presented. We assume that system (1) is invertible, and that input-output inversion can be achieved via purely static state feedback of the form

$$\mathbf{u} = \alpha(\mathbf{x}) + \beta(\mathbf{x})\mathbf{v}, \qquad \text{with } \beta(\mathbf{x}) \text{ nonsingular.} \tag{5}$$

In this case, one can take in the first place the compensated system constituted by the original plant under the action of the above inversion feedback. A proper change of coordinates $\tilde{\mathbf{x}} = \Psi(\mathbf{x})$, with $\Psi(\mathbf{0}) = \mathbf{0}$, displays the linearity of input-output paths in the compensated system. The synthesis of a regulator can then be performed on the external side of (5), applying the direct design to the new input $\mathbf{v}$. As a result, the control law fed into the original plant

$$\mathbf{u} = \alpha(\mathbf{x}) + \beta(\mathbf{x})\big(\tilde{\mathbf{c}}(\mathbf{w}) + \tilde{\mathbf{F}}(\tilde{\mathbf{x}} - \tilde{\pi}(\mathbf{w}))\big) \tag{6}$$

is a nonlinear state feedback, making the transformed manifold $\tilde{\mathbf{x}} = \tilde{\pi}(\mathbf{w})$ attractive. Figure 2 shows the overall block diagram of this *indirect* regulator. In order to assign the same eigenvalues specified by $\mathbf{F}$ in (3) to the linear approximation at $\tilde{\mathbf{x}} = \mathbf{0}$ of the compensated system, the linear feedback matrix in (6) should be chosen as

$$\tilde{\mathbf{F}} = \beta^{-1}(\mathbf{0})(\mathbf{F} - \alpha_{\mathbf{x}}(\mathbf{0}))\Psi_{\mathbf{x}}^{-1}(\mathbf{0}), \tag{7}$$

where a subscript denotes the Jacobian of the relative mapping.

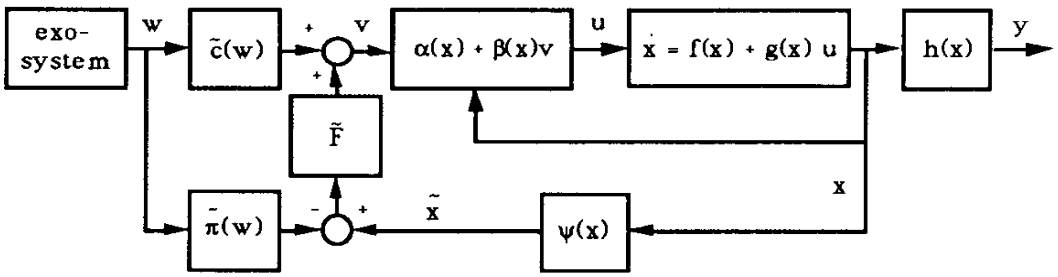

Fig. 2 — Nonlinear regulator: indirect design

The motivation for a two-stage approach stands in the benefits obtained by (5), which typically cancels the 'heavy' nonlinearities present in the original system. For example, in the case of robots with multiple flexible links, use of an inversion feedback results in complete compensation of all nonlinear rigid body effects, which dominate the 'slow' dynamics of the system. As a consequence, the explicit derivation of an indirect regulator, namely the computation of $\tilde{\mathbf{c}}(\mathbf{w})$ and $\tilde{\pi}(\mathbf{w})$ solving equations similar to (4) for the compensated system, turns out to be easier and numerically more robust than in the direct case. This observation is strengthened when approximate computations are introduced. On the other hand, system (1) may have been driven to instability through the application of (5). Yet, the regulator will take care of induced unstable behaviors since the same approach works also for an unstable plant, as long as it is stabilizable. Note also that the compensated system can still be stabilized by linear feedback.

Exploitation of system invertibility, which led to (6), can be combined with the simplicity of control law (3), where all model nonlinearities are taken into account in the feedforward term. To this end, regulation may be obtained using the same control structure as in (6), but evaluating nonlinear terms at their values on the manifold $\mathbf{x} = \pi(\mathbf{w})$, instead of at their current ones. The control input becomes

$$\mathbf{u} = \alpha(\pi(\mathbf{w})) + \beta(\pi(\mathbf{w}))\big(\tilde{\mathbf{c}}(\mathbf{w}) + \hat{\mathbf{F}}(\mathbf{x} - \pi(\mathbf{w}))\big). \tag{8}$$

Since feedforward terms in (3) and (8) must be equal, the following relation holds:

$$\mathbf{c}(\mathbf{w}) = \alpha(\pi(\mathbf{w})) + \beta(\pi(\mathbf{w}))\tilde{\mathbf{c}}(\mathbf{w}). \tag{9}$$

This stresses the internal structure of the feedforward part of regulators, in the case of invertible systems. As for the linear feedback term, stabilization is obtained by means of a constant $\mathbf{F}$ in the direct design, while the mixed design achieves pole placement using a time-varying matrix $\beta(\pi(\mathbf{w}))\hat{\mathbf{F}}$. Close to the steady-state manifold, this gain modulation is expected to be superior to constant linear feedback. In the robotic case, this is roughly equivalent to weighting the feedback gain by the 'apparent' rigid inertia matrix.

The three proposed schemes are different regulators designed for the stable tracking of output trajectories in nonlinear systems. In case of matched initial conditions, $\mathbf{x}(0) = \pi(\mathbf{w}(0))$ viz. $\tilde{\mathbf{x}}(0) = \tilde{\pi}(\mathbf{w}(0))$, exact trajectory reproduction is obtained, and (3), (6), and (8) collapse into a unique feedforward law that assigns the same steady-state behavior. When matching of the full initial state is impractical, only asymptotic tracking is possible and the above control laws will produce different transient behaviors: in this respect, the best performance is achieved with the indirect approach. On the other hand, control laws (3) and (8) are simpler, because most of the computations can be done off line.

A One-Link Flexible Arm Model

A one-link flexible planar robot arm will be used as a case study for the end-effector tracking problem. A simple modeling technique divides the flexible link into rigid segments that are connected by elastic springs, where link deformation is concentrated. Following the Lagrangian approach, a nonlinear dynamic model can be obtained in the standard form. Explicit expressions that are parametrized in the number of segments have been derived in [12], so that model order can be varied easily to achieve the prescribed accuracy. The following treatment will be limited to the case of two equal segments of uniform mass, moving on the horizontal plane. Let m and ℓ denote the total link mass and length, k the spring elasticity, u the input torque, θ_1 the angular position of the link base, and θ_2 the flexible variable. The dynamic equations are

$$\begin{bmatrix} b_{11}(\theta_2) & b_{12}(\theta_2) \\ b_{12}(\theta_2) & b_{22} \end{bmatrix} \begin{bmatrix} \ddot{\theta}_1 \\ \ddot{\theta}_2 \end{bmatrix} + \begin{bmatrix} c_1(\theta_2, \dot{\theta}_1, \dot{\theta}_2) + d_1\dot{\theta}_1 \\ c_2(\theta_2, \dot{\theta}_1) + k\theta_2 + d_2\dot{\theta}_2 \end{bmatrix} = \begin{bmatrix} 1 \\ 0 \end{bmatrix} u, \tag{10}$$

with the elements of the inertia matrix $B(\theta_2)$ given by

$$b_{11}(\theta_2) = a + 2c\cos\theta_2, \quad b_{12}(\theta_2) = b + c\cos\theta_2, \quad b_{22} = b,$$

and Coriolis and centrifugal terms

$$c_1(\theta_2, \dot{\theta}_1, \dot{\theta}_2) = -c\,(\dot{\theta}_2^2 + 2\dot{\theta}_1\dot{\theta}_2)\sin\theta_2, \quad c_2(\theta_2, \dot{\theta}_1) = c\,\dot{\theta}_1^2\sin\theta_2,$$

where $a = 5m\ell^2/24$, $b = m\ell^2/24$, $c = m\ell^2/16$. In (10), d_1 and d_2 are damping coefficients representing viscous friction at the joint and link structural (passive) dissipation, respectively. State equations can be obtained by setting $\mathbf{x} = (\theta_1, \theta_2, \dot{\theta}_1, \dot{\theta}_2) \in \mathbb{R}^4$, but we will keep the second-order differential representation for compactness. The linearized expression of the end-effector angular position, as seen from the base,

$$y = \theta_1 + \frac{1}{2}\theta_2 \tag{11}$$

will be taken as controlled output for the system. The above finite-dimensional model, although of reduced-order, displays the same basic control properties of more accurate and complex distributed models.

Indirect Nonlinear Regulator Design

In order to obtain output tracking of end-effector trajectories for the considered one-link flexible arm, we will follow the indirect nonlinear regulator design. Stabilizability of the linear approximation of (10) around the origin $\mathbf{x} = \mathbf{0}$ is easily verified. Since the relative degree of output (11) is two, the synthesis of an inversion-based control is accomplished by deriving twice the output and setting $\ddot{y} = v$. Solving for u yields

$$u = c_1(\theta_2, \dot{\theta}_1, \dot{\theta}_2) + d_1\dot{\theta}_1 + \frac{b_{11}(\theta_2) - 2b_{12}(\theta_2)}{2b_{22} - b_{12}(\theta_2)}(c_2(\theta_2, \dot{\theta}_1) + k\theta_2 + d_2\dot{\theta}_2) + \frac{2\det B(\theta_2)}{2b_{22} - b_{12}(\theta_2)} v = \alpha(\mathbf{x}) + \beta(\mathbf{x})v. \tag{12}$$

In the system after inversion, the input-output linearizing coordinates are $\widetilde{\mathbf{x}} = (y, \dot{y}, \theta_2, \dot{\theta}_2)$. In view of (11), here $\Psi(\mathbf{x})$ is just a linear transformation in the state space. The closed-loop equations can be written as

$$\begin{aligned} \ddot{y} &= v, \\ \ddot{\theta}_2 &= \frac{2(c_2(\dot{y}, \theta_2, \dot{\theta}_2) + k\theta_2 + d_2\dot{\theta}_2)}{b_{12}(\theta_2) - 2b_{22}} + \frac{2b_{12}(\theta_2)}{b_{12}(\theta_2) - 2b_{22}} v = \gamma(\widetilde{\mathbf{x}}) + \delta(\widetilde{\mathbf{x}})v. \end{aligned} \tag{13}$$

The zero-dynamics of the system is then obtained by setting $y(t) \equiv 0$ [6]:

$$\ddot{\theta}_2 = -\frac{(c/2)\dot{\theta}_2^2 \sin\theta_2 + 2(k\theta_2 + d_2\dot{\theta}_2)}{b - c\cos\theta_2}. \tag{14}$$

It is easy to see that this two-dimensional dynamics is unstable in the first approximation. Therefore, tracking of a desired output trajectory $y_d(t)$ cannot be achieved by simply stabilizing the (linear) input-output behavior in (13), i.e. using

$$v = \ddot{y}_d + \widetilde{F}_1(y - y_d) + \widetilde{F}_2(\dot{y} - \dot{y}_d), \qquad \widetilde{F}_1, \widetilde{F}_2 < 0, \tag{15}$$

as specified in a pure inversion-based approach [1,2]. As a matter of fact, (15) will force the state of the system to become unbounded. This is always true, except for particular initial conditions which depend on the desired trajectory. The initial state which guarantees — at least in principle — an overall bounded evolution is given by the steady-state trajectory $\widetilde{\pi}(\mathbf{w}(t))$, evaluated at time $t = 0$. This computation is a by-product of the regulator derivation and it has to be performed according to the specific reference trajectory, being the state $\mathbf{w}$ of the exosystem inherently related to the desired output evolution. Note that, if the flexible arm is in a different initial state, *only* the regulator approach will be capable of achieving asymptotic output tracking with bounded internal state. However, if a non-causal solution is admitted [11], one may compute an input torque for $t < 0$, i.e. to be applied before the trajectory starts, in such a way to bring the system at time $t = 0$ on the steady-state manifold.

We will first consider how to obtain $\widetilde{c}(\mathbf{w})$ and $\widetilde{\pi}(\mathbf{w})$ for a *cubic spline* reference trajectory $y_d(t) = r_3t^3 + r_2t^2 + r_1t + r_0$. This can be generated by a properly initialized linear exosystem in Brunovski canonical form of order four: $\dot{w}_i = w_{i+1}$, $i = 1, \ldots, 3$, $\dot{w}_4 = 0$, $y_d = w_1$. Accordingly, the initial state of the exosystem should be $\mathbf{w}(0) = (r_0, r_1, 2r_2, 6r_3)$. This chain structure of integrators can be extended to the nth order for generating, as y_d, polynomial trajectories of degree $n - 1$. Here, the important point to remark is that these exosystems are *not* even stable for $n \geq 2$. If an infinite time horizon is considered, any of these polynomial trajectories will become unbounded. However, the proper initialization of these exosystems and the limited time span considered in typical robotic applications allows to overcome this critical point. In the cubic case, the most practical choice is to set a finite time t_f, specifying initial and final position and velocity (typically, zero). For $y_d(0) = y_0$, $\dot{y}_d(0) = y_0'$, $y_d(t_f) = y_f$, $\dot{y}_d(t_f) = y_f'$, the spline coefficients take on the values:

$$\begin{bmatrix} r_3 \\ r_2 \end{bmatrix} = \frac{1}{t_f^3} \begin{bmatrix} -2(y_f - y_0) + t_f(y_f' + y_0') \\ 3t_f(y_f - y_0) - t_f^2(y_f' + 2y_0') \end{bmatrix}, \qquad \begin{bmatrix} r_1 \\ r_0 \end{bmatrix} = \begin{bmatrix} y_0' \\ y_0 \end{bmatrix}. \tag{16}$$

Taking advantage of the structure of system (13), equations (4) particularize to

$$\widetilde{\pi}_1(\mathbf{w}) = w_1, \qquad \widetilde{\pi}_2(\mathbf{w}) = w_2, \qquad \widetilde{c}(\mathbf{w}) = w_3, \tag{17}$$

and, hence, to the following reduced set of partial differential equations

$$\frac{\partial \widetilde{\pi}_3}{\partial w_1} w_2 + \frac{\partial \widetilde{\pi}_3}{\partial w_2} w_3 + \frac{\partial \widetilde{\pi}_3}{\partial w_3} w_4 = \widetilde{\pi}_4(\mathbf{w}), \tag{18a}$$

$$\frac{\partial \widetilde{\pi}_4}{\partial w_1} w_2 + \frac{\partial \widetilde{\pi}_4}{\partial w_2} w_3 + \frac{\partial \widetilde{\pi}_4}{\partial w_3} w_4 = \gamma(\widetilde{\pi}(\mathbf{w})) + \delta(\widetilde{\pi}(\mathbf{w}))w_3, \tag{18b}$$

with the γ and δ functions defined in (13). As expected, the first two components of the steady-state behavior $\widetilde{\pi}(\mathbf{w})$ are the output reference position and velocity, while the feedforward term $\widetilde{c}(\mathbf{w})$ is just the desired output acceleration. Equations (18) can be solved approximately using polynomial expansion. In particular, because of the second-order nature of the underlying mechanical system, it is sufficient to choose an approximation for $\widetilde{\pi}_3(\mathbf{w})$. Then, $\widetilde{\pi}_4(\mathbf{w})$ will follow immediately from (18a). Considering a complete third order polynomial expression for $\widetilde{\pi}_3(\mathbf{w})$, substitution into (18b), Taylor expansion of the nonlinear terms (up to third order), and final application of the identity principle of polynomials gives

$$\begin{aligned}\widetilde{\pi}_3(\mathbf{w}) = {} & a_3 w_3 + a_4 w_4 + w_2^2(a_{223} w_3 + a_{224} w_4) + a_{234} w_2 w_3 w_4 + a_{333} w_3^3 \\ & + w_3^2(a_{233} w_2 + a_{334} w_4) + w_4^2(a_{244} w_2 + a_{344} w_3) + a_{444} w_4^3,\end{aligned} \tag{19}$$

with definite values of the nonzero coefficients appearing in (19). Incidentally, note that a 'linear' version of the regulator can be obtained within the present framework, by limiting the above expansions to first order terms. With these computed expressions, the resulting v will be of the form

$$v = \widetilde{c}(\mathbf{w}) + \widetilde{\mathbf{F}} \begin{bmatrix} y - \widetilde{\pi}_1(\mathbf{w}) \\ \dot{y} - \widetilde{\pi}_2(\mathbf{w}) \\ \theta_2 - \widetilde{\pi}_3(\mathbf{w}) \\ \dot{\theta}_2 - \widetilde{\pi}_4(\mathbf{w}) \end{bmatrix} = \ddot{y}_d + \widetilde{\mathbf{F}} \begin{bmatrix} y - y_d \\ \dot{y} - \dot{y}_d \\ \theta_2 - \widetilde{\pi}_3(\dot{y}_d, \ddot{y}_d, \dddot{y}_d) \\ \dot{\theta}_2 - \widetilde{\pi}_4(\dot{y}_d, \ddot{y}_d, \dddot{y}_d) \end{bmatrix}, \tag{20}$$

which should be compared to (15), as a clear distinction between the two of approaches of inversion and regulation. Combining (20) with (12) gives the actual input torque applied to the flexible robot arm.

As a second simple example of computation of the terms $\widetilde{c}(\mathbf{w})$ and $\widetilde{\pi}(\mathbf{w})$, we take the classical *point-to-point* (rest-to-rest) move. In this case, a scalar exosystem is defined as $\dot{w} = 0$, $w(0) = y_f$, $y_d(t) = w$, and the indirect regulator design provides

$$\widetilde{c}(w) = 0, \qquad \widetilde{\pi}_1(w) = w = y_f, \qquad \widetilde{\pi}_2(w) = \widetilde{\pi}_3(w) = \widetilde{\pi}_4(w) = 0. \tag{21}$$

Simulation Results

The proposed nonlinear regulator was tested by simulation using as parameters for the one-link flexible arm $\ell = 1$ m, $m = 0.2$ kg, $k = 5$ Nm/rad, and $d_1 = d_2 = 0.01$ Nm sec/rad. Simulations were run using Matlab, with a fourth order Runge-Kutta integration method.

For the spline trajectory, the following data were used: $y_0 = 0°$, $y_f = 90°$, $y_0' = y_f' = 0$, $t_f = 1$ sec, with the feedback matrix $\widetilde{\mathbf{F}}$ assigning poles at $-20 \pm i30$ and $-30 \pm i25$ to the linearized system. Figures 3–7 show the obtained tracking results. In particular, note that the maximum error during transients is very limited (0.6° in Fig. 4). The presence of transient errors, even if the output is initially matched with the desired one, is due to the fact that the arm starts from rest in its undeformed condition ($\theta_2 = \dot{\theta}_2 = 0$). Instead, initial belonging to the steady-state manifold would require e.g. $\theta_2(0)$ to be equal to

$$\widetilde{\pi}_3(\mathbf{w}(0)) = \frac{6y_f}{t_f^2}\left(a_3 - \frac{2}{t_f} a_4\right) + \frac{216\, y_f^3}{t_f^6}\left(a_{333} - \frac{2}{t_f} a_{334} + \frac{4}{t_f^2} a_{344} - \frac{8}{t_f^3} a_{444}\right) \neq 0. \tag{22}$$

A 'dual' mismatched situation occurs at the trajectory end, after t_f. In Fig. 5, the non-minimum phase behavior of the tip is shown by its reversed initial velocity, as opposed

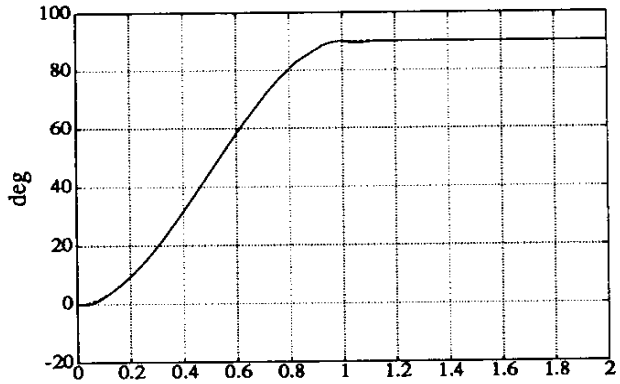

Fig. 3 - Output tracking of a spline trajectory

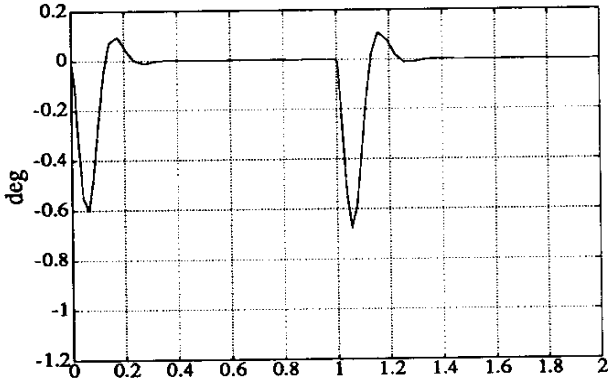

Fig. 4 - Tip error on the spline

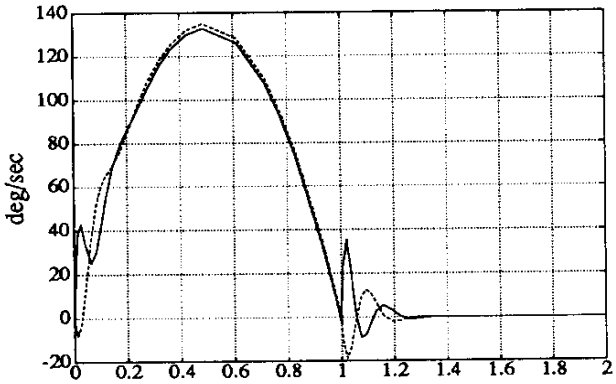

Fig. 5 - Tip (---) and joint velocity on the spline

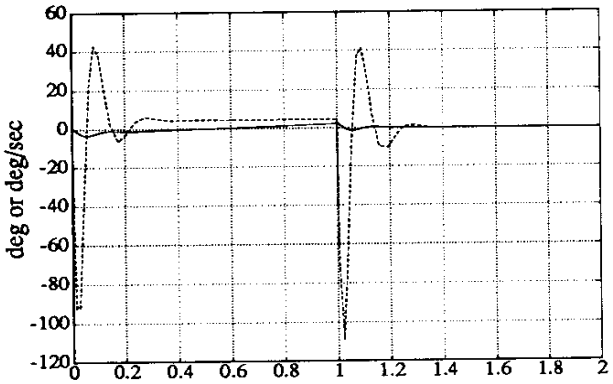

Fig. 6 - Link deflection and derivative (---) on the spline

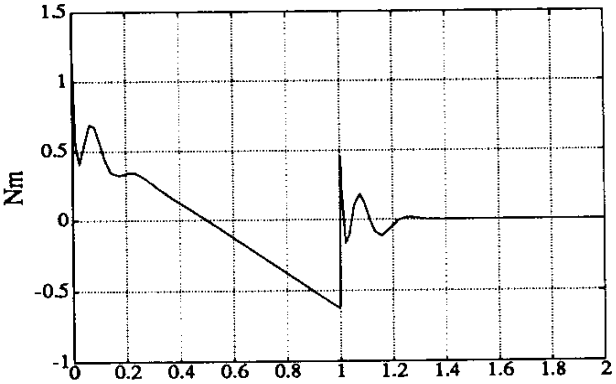

Fig. 7 - Input torque on the spline

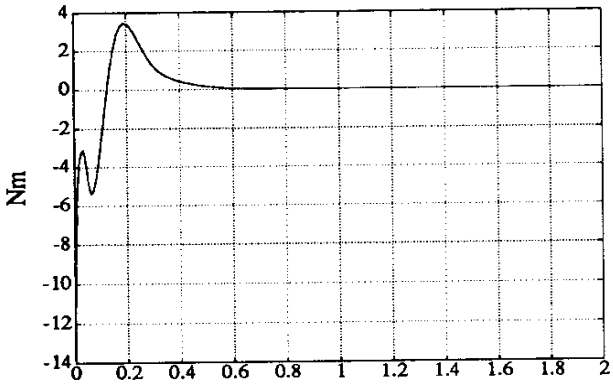

Fig. 8 - Point to point regulation: input torque

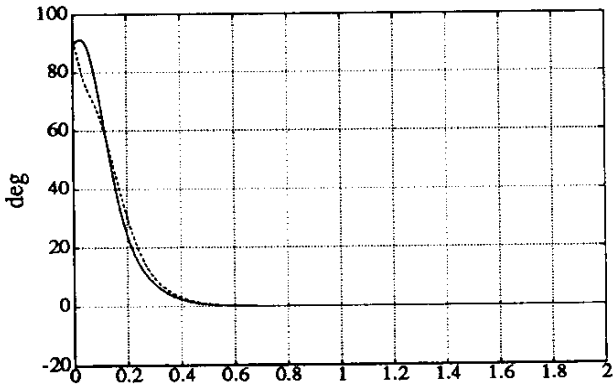

Fig. 9 - Point to point regulation: joint (---) and tip angle

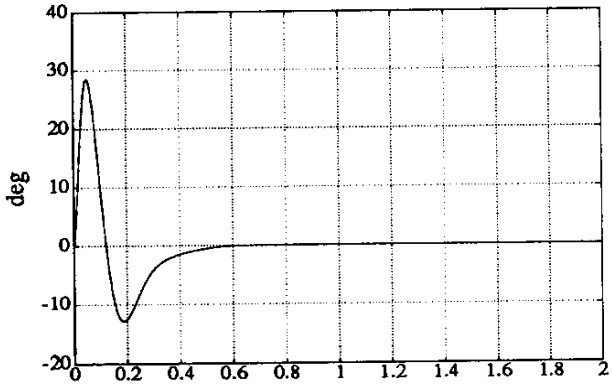

Fig. 10 - Point to point regulation: link deflection

to joint velocity. One can also note from Fig. 6 that the link deflection θ_2 is slightly but constantly increasing during motion. This is due to the linear growth of the spline acceleration, which would force over time an extremely large deformation into the system. Nevertheless, the deflection remains limited and reaches a peak value of 5°. The applied torque u in Fig. 7 follows closely the equivalent rigid one. These results are quantitatively similar to the ones obtained in [12] with an harmonic exosystem (which is Poisson stable).

The same total net motion ($y_0 = 90°$, $y_f = 0°$) was considered for point-to-point regulation, with double real poles assigned by $\widetilde{\mathbf{F}}$ at -20 and -30. Figures 8–10 show that the nonlinear regulator achieves the rest-to-rest task in only 0.6 sec, but with a larger torque effort and a link deflection which is five times times as large as in the spline motion. Since $\widetilde{\pi}_3$ and $\widetilde{\pi}_4$ are zero in this case, the resulting input signal in (20) executes also what is usually called a 'modal damping' action, e.g. in the form $\widetilde{F}_3\theta_2 + \widetilde{F}_4\dot{\theta}_2$. However, the benefit of this conventional strategy becomes questionable for general trajectory tracking in flexible structures, when the natural steady-state deflection is different from zero.

Conclusions

The problem of tracking end-effector trajectories in a flexible robot arm is conveniently solved via nonlinear regulation theory. Different possible realizations of nonlinear regulators have been presented, highlighting achievable tracking accuracy and ease of implementation. It was shown in simulation how trajectories generated by exosystems not belonging to the theoretical framework worked out until now can still be asymptotically tracked with very satisfactory results. The improvements gained with the nonlinear approach over linear tracking regulators have already been shown in [12].

References

[1] R.M. Hirschorn, "Output tracking in multivariable nonlinear systems," *IEEE Trans. on Automatic Control*, vol. AC-26, no. 2, pp. 593–595, 1981.

[2] S.N. Singh, "Generalized functional reproducibility condition for nonlinear systems," *IEEE Trans. on Automatic Control*, vol. AC-27, no. 4, pp. 958–960, 1982.

[3] T.J. Tarn, A.K. Bejczy, A. Isidori, and Y. Chen, "Nonlinear feedback in robot arm control," *Proc. 23rd Conf. on Decision and Control* (Las Vegas, NV, Dec. 12–14, 1984), pp. 736–751.

[4] A. De Luca, "Dynamic control of robots with joint elasticity," *Proc. 1988 IEEE Int. Conf. on Robotics and Automation* (Philadelphia, PA, Apr. 24–29, 1988), pp. 152–158.

[5] A. Isidori, C.H. Moog, and A. De Luca, "A sufficient condition for full linearization via dynamic state feedback," *Proc. 25th IEEE Conf. on Decision and Control* (Athens, GR, Dec. 10–12, 1986), pp. 203–208.

[6] C. Byrnes and A. Isidori, "Local stabilization of critically minimum phase nonlinear systems," *Systems and Control Lett.*, vol. 11, no. 1, pp. 9–17, 1988.

[7] A. Isidori and C. Byrnes, "Output regulation of nonlinear systems," *IEEE Trans. on Automatic Control*, vol. AC-35, no. 2, pp. 131–140, 1990.

[8] A. De Luca and B. Siciliano, "Joint-based control of a non-linear of a flexible arm," *Proc. 1988 American Control Conf.* (Atlanta, GA, Jun. 15–17, 1988), pp. 935–940.

[9] R.H. Cannon, Jr. and E. Schmitz, "Initial experiments on the end-point control of a flexible one-link robot," *Int. J. of Robotics Research*, vol. 3, no. 3, pp. 62–75, 1984.

[10] A. De Luca, P. Lucibello, and G. Ulivi, "Inversion techniques for trajectory control of flexible robot arms," *J. of Robotic Systems*, vol. 6, no. 4, pp. 325–344, 1989.

[11] E. Bayo, "A finite-element approach to control the end-point motion of a single-link flexible robot," *J. of Robotic Systems*, vol. 4, no. 1, pp. 63–75, 1985.

[12] A. De Luca, L. Lanari, and G. Ulivi, "Output regulation of a flexible robot arm," *Proc. 9th INRIA Int. Conf. on Analysis and Optimization of Systems* (Antibes, F, Jun. 12–15, 1990), pp. 833–842.

Alessandro De Luca, Leonardo Lanari, Giovanni Ulivi

Dipartimento di Informatica e Sistemistica
Università degli Studi di Roma "La Sapienza"
Via Eudossiana 18, 00184 Roma, Italy

This paper is based on work supported by the *Consiglio Nazionale delle Ricerche*, grant no. 90.00381.PF67 (*Progetto Finalizzato Robotica*).